TITLE OF THE PROJECT: "Research on CdZnTe and other novel room temperature gamma ray spectrometer materials" by

Arnold Burger (PI), Michael Groza, Yunlong Cui, Utpal N. Roy, and M. Guo
Department of Physics, Fisk University, Nashville, TN 37208, U.S.A.

Final Report

Grant number: DE-FG07-04ID14555
Fisk acct. #: 2109
Submitted to: Procurement Services Division, Idaho Operations Office
in support of
US DOE - Office of Nonproliferation Research and Engineering
Office of Defense Nuclear Nonproliferation
National Nuclear Security Administration (NA-22)

Period covered: Feb 23, 2004 - Feb 22, 2007 Due date: 5/24/2007

Technical Point of Contact:

Arnold Burger, PhD
Principal Investigator
1000 17th Ave. N.
Department of Physics
Fisk University
Nashville, TN 37208-3051

Ph.: 615-329-8516
FAX: 615-329-8634
E-mail: aburger@fisk.edu

Administrative Point of Contact:

Thelma Jackson
Account Manager
1000 17th Ave. N.
Dubois Hall, Rm. 245
Fisk University
Nashville, TN 37208-3051

Ph.: 615-329-8705
FAX: 615-329-8634
E-mail: tjackson@fisk.edu

Abstract
Room temperature gamma-ray spectrometers are being developed for a number for years for national security applications where high sensitivity, low operating power and compactness are indispensable. The technology has matured now to the point where large volume (several cubic centimeters) and high energy resolution (approximately 1% at 660 eV) of gamma photons, are becoming available for their incorporation into portable systems for remote sensing of signatures from nuclear materials.

The dependence of electron mobility-lifetime product ($\mu\tau$) and surface recombination velocity (S/μ) on surface processing and temperature for $Cd_{1-x}Zn_xTe$ (CZT) radiation detectors is studied. The surfaces of the CZT crystals were treated with mechanical polishing followed by 2% bromine-in-methanol chemical etching. Different regions at the Au contacts were illuminated with light at a wavelength of 650, 800 900 and 940 nm. The position-dependent and temperature-

dependent values of the electron mobility–lifetime product and surface recombination velocity were measured using a direct current (DC) photoconductivity technique. The study reveals that the DC photoconductivity technique is a practical method to measure the spatial and temperature variations of the surface recombination velocity and bulk lifetime for CZT detectors. The correlation of the DC photoconductivity and detector performance measurements is discussed.

The Fisk research group is developing unique and dedicated characterization tools to determine the limiting performance factors any stage in the material development.

Primarily we are focusing on CdZnTe research and we make available these tools to all other researchers funded by NNSA/NA-22.

1. Introduction

$Cd_{1-x}Zn_xTe$ (CZT) is a promising semiconductor material for room temperature x-ray and gamma-ray spectroscopy applications. Studies of the spatial and temperature dependences of the electron lifetimes and surface recombination velocities of CZT detectors are helpful to understand the detector performances and its correlation with material inhomogeneities. Variations of composition and imperfections during crystal growth and device processing result in non-uniformities in the electron generation rate and carrier transport, which adversely affect the detector performance. Toney et al.[1] have studied compositional variations in CZT using low-temperature photoluminescence spectroscopy and room-temperature photoluminescence mapping. Amman et al.[2] characterized CZT crystals using alpha particle response, and they found a correlation between the alpha response map and the distribution of tellurium inclusions. Recently, Sturm et al.[3] studied the spectroscopic performance of CZT for reduced temperature and observed degraded performance for temperatures below 0°C and a complete loss of spectral information at -30°C.

It has been reported that the surface effects can play an important role in CZT detector performance.[4-5] For a CZT detector excited by either an alpha particle or above bandgap light, the electron-hole pairs are generated within a thin layer (~1 μm) near the surface of the crystal. Therefore, surface effects such as the metal contacts, mechanical polishing and chemical etching, should be taken into account for many measurement techniques. Typically, the effects of surface quality and contact issues have not been included in the data analysis, which casts some doubt on the values for mobility-lifetime as reported by many investigators. In this paper, we studied the variation of the electron mobility-lifetime product, as well as surface recombination velocity, on the surface quality and excitation conditions of CZT detectors. The CZT detectors had Au contacts, and the surfaces were treated with a 2% bromine-in-methanol etching solution. Different regions at the cathode were illuminated with light having a wavelength of 650, 800, 900 and 940 nm. With 650-nm light illumination, the photons are mainly absorbed near the surface of the crystal, and values for the electron generation rate and transport are greatly affected by the surface condition. With illumination by 800-nm light, which is close to the energy gap between conduction and valence band of CZT crystal, most of the light is absorbed within the bulk of crystal. Here, the bulk material properties dominate the electron generation rate and transport. With illumination by light with wavelength at 900-nm or higher, the light is weakly absorbed through the crystal, and the ionization of traps dominates the electron properties. For a uniform concentration of neutral trap levels within the bulk, the generation rate will also be uniform. The values of the electron mobility–lifetime product and surface recombination velocity are measured using a DC photoconductivity technique for samples with different surface

processing conditions. The technique is a relatively simple method to precisely map both the electron lifetime and surface recombination velocity. Furthermore, it is easy to combine the low-temperature DC photoconductivity with low-temperature PL measurements in the same experimental setup, which provides a practical way to correlate variations of the $\mu\tau$ value.

2. ACHIEVEMENTS in the project

a) Detector Fabrication and Testing

A new lab with photolithography equipment in a class 10,000 clean room facility was established at Fisk where the fabrication of CZT samples was performed. The surface leakage, the surface recombination velocity and gamma-ray performances of CZT crystals have been shown to be dramatically modified by the choice of chemical etchant. In particular, surface chemistry studies and development of procedures for passivation and implemented to limit surface leakage currents which are now necessary steps in fabrication. It appears that in some cases the chemical etching with a bromine-methanol solution can be skipped, with little effects on the spectroscopic performance, and in this case as-polished surface may exhibit a crystallographic polarity effect although more studies are needed.

In Fig. 1 we show the effect the presence of an oxide layer under one of the electrodes. The internal electric field was measured and mapped using infrared microscopy of the Pockels electro-optic effect. In practice, both intentional and unintentional oxide layers on CZT surfaces can be encountered, and this fact indicates the need for taking into account the surface effects in future modeling and designing of devices. These data are important to be understood and either employed in a useful manner in future detector fabrication, or prevented in cases where the distortion of the internal electric field would have a deleterious effect.

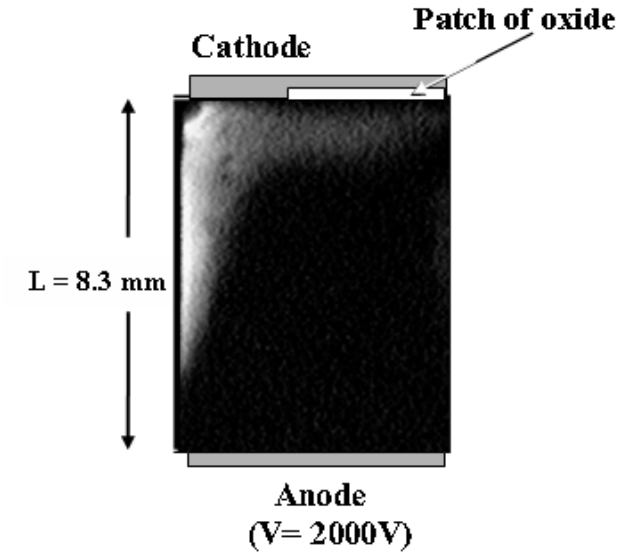

Fig. 1 The modification of the internal electric field when an oxide layer was intentionally placed partially under one of the electrodes. The photo was obtained utilizing the infrared microscopy of the Pockels effect . Lighter areas indicate a stronger electric field.

Two particular types of detectors were fabricated and tested in this study, (i) a CZT Frisch capacitive grid, and (ii) a 4x4 pixelated device. The Frisch capacitive (insulated) grid (inventor Douglas McGregor – KSU) is a device that has one of the simplest approaches achieving near single-carrier performance. The readout electronics is based on a standard charge sensitive preamplifier.

Bar-shaped geometries, with the field applied lengthwise, have been found to be optimal, although in the present study we have preferred to use a cube geometry and refabricate the Frisch capacitive grid configurations along the three directions, and measure their performance for the two polarities of the bias. The grid, made of 40 micron thick copper foil, could be adjusted for length, and could slide to maintain a similar geometry for both polarities. A layer of 40 micron thick Kapton® was used as dielectric between the copper grid and the CZT crystal. One of the configurations tested is shown in Fig.2 Peak-to-Compton ratios raging between 0.5 to 2 could be measured in response to 662 keV gammas emitted by a 137Cs source, for an identical grid geometry. Thus, we have determined again the possibility that factors such as crystallographic orientation and polarity might play a role in the optimization of such a device and may account for past cases where different results were obtained by two groups on the same crystal. Figure 3 presents one of the better spectra from a capacitive Frisch grid device in response to 137Cs illumination, obtained in this study.

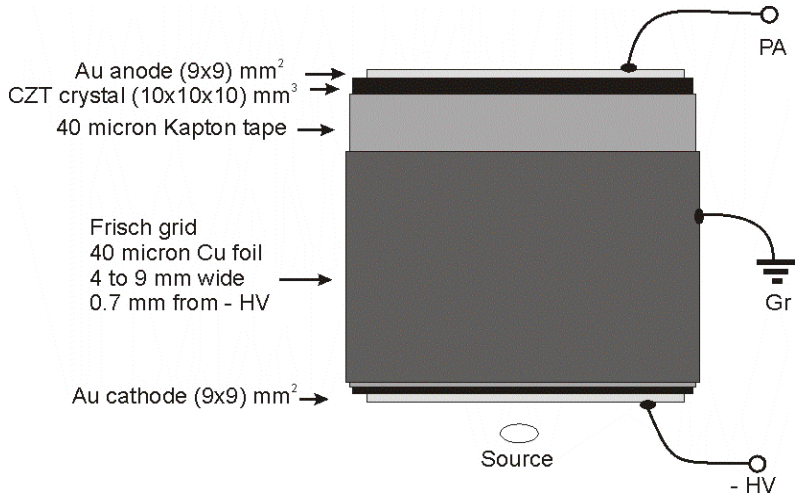

Fig. 2 Schematic diagram of a three terminal CZT Frisch capacitive grid.

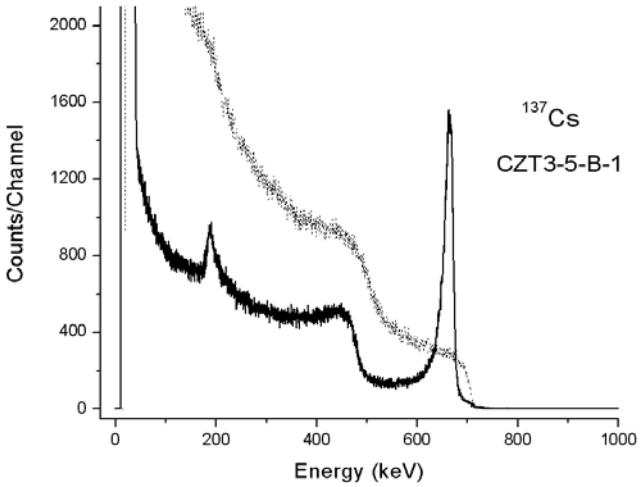

Fig. 3 The response of the same CZT crystal (11X11X11 mm3) to 137Cs in the planar configuration (dashed line) and with a Frisch capacitive grid (solid line). The FWHM at 662 keV is FWHM=17.8 keV (2.7%) with an electronic noise contribution of 4.5 keV.

A pixelated detector (11x11x11mm^3) was fabricated by Fisk from ingot CZT3-4 (Figure 3). The pixilated (4x4) detector utilizes the small pixel effect and acts like an electron-transport-only device. A FWHM value of 1.35% at 662 keV was obtained. This value was measured using low-quality preamps, which exhibited relatively high noise. With better electronics, values for the FWHM of up to 1.14% at 662 keV were obtained. The fabrication of the detector, the development of the electronic read-out (16-channels) and the device testing were performed at Fisk. Brookhaven National Laboratory provided the mask for the metal (Au) contacts deposition performed by RF sputtering.

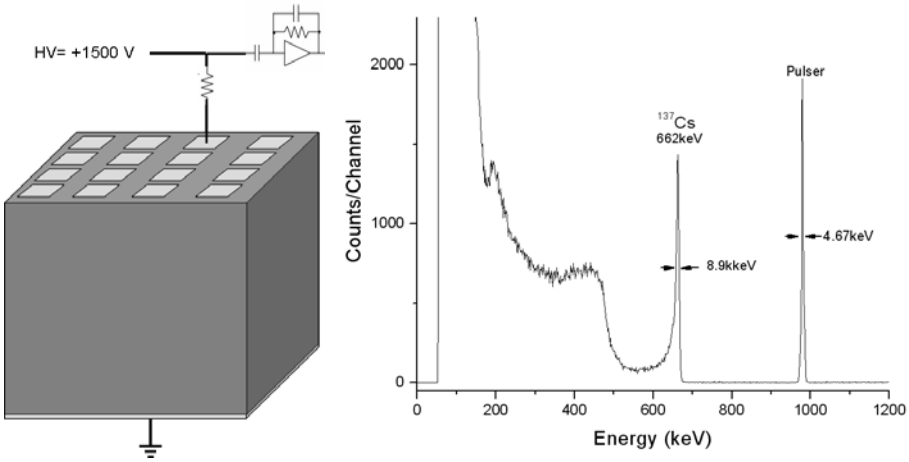

Fig. 4 The response of one of the pixels (2.2..2X2.2 mm2, top row, third from left) of a 4 x 4 pixels CZT detector crystal (1.1x1.1X1.1 cm3) to 137Cs source yielding an energy resolution of 1.35% at 662 keV. The applied bias was -1600 V.

Detector-grade CZT crystals with dimensions of 6.4×6.4×4.7 mm^3 (sample 1) and 7.0×7.0×3.9 mm^3 (sample 2) were obtained from eV Products, Inc. Samples 1 and 2 were prepared for measurements of position variation at room temperature and temperature variation of $\mu\tau$ and S/μ, respectively. The crystals were grown by the high-pressure Bridgman technique. Two surfaces of

sample 1 were labeled as surface A and B, respectively. The crystals were polished on a mechanical polisher with 0.05-μm particle size alumina suspension and rinsed in methanol, then treated in 2% bromine-in-methanol (BM) etching solution for two minutes. Au contacts were sputtered using 50-W radio frequency power in a 6.7-Pa argon pressure, then Pd wires were attached to the Au contacts using a colloidal graphite suspension in water. Finally, the devices were covered with a protective Humiseal coating. At least six different regions of each surface of sample 1 were selected for illumination. Fig. 1 shows the six selected regions, where area 1 is located at the top center of the surface, area 2 at top right, area 3 at the center, area 4 at center right, area 5 at bottom center, and area 6 at bottom right. For surfaces A and B, Pd wires were placed at the bottom left and top left corners, respectively. Details of the experimental setup for the DC photocurrent and detector performance measurements have been reported elsewhere. [6-7] DC photocurrent measurements were carried out with a custom-made computer-interfaced system. A temperature between 250 K and 300 K was set by a MMR micro-miniature refrigeration system coupled to a K-20 programmable temperature controller. Light with a wavelength λ = 650, 800, 900 and 940 nm was used for the illumination. The illuminated area had a size of 2 mm^2 for all data reported in this paper. The detector performance was evaluated with ^{241}Am point sources. The 5.5-MeV α particle and 59.6-keV gamma-ray photopeaks associated with ^{241}Am emissions were measured as a function of the applied voltage bias. The peaking time of the system was varied to optimize tradeoffs between the charge collection and noise due to leakage currents.

b) Photoconductivity studies and improved surface preparation

For 650-nm light illumination, as pointed out in our previous article, the surface recombination velocity is found to be a function of the illumination intensity.[6] As the intensity and accompanied electron generation rate were increased, the surface recombination velocity was also found to increase.

For the experiments reported in this paper, the light power was kept constant at a low level. The experimental data was found to fit the equation: [6]

$$I = \frac{I_0}{1 + LVS/\mu} \mu\tau_b V / L^2 [1 - \exp(-L^2/(\mu\tau_b V))] \quad . \qquad (1)$$

Here, L is the detector thickness, V is the applied bias, μ is the electron mobility, and τ_b is electron bulk lifetime. I_0 is the saturation photocurrent, which is proportional to the electron generation rate. The equation becomes the Hecht equation for S=0 (i.e., no surface recombination). It is found that the saturation photocurrent I_0 for 650-nm excitation is slightly different. The small difference of I_0 is attributed to the different electron generation rates. At regions 2, 3 and 4, the $\mu\tau_b$ values are 1.9×10^{-2}, 1.7×10^{-2} and 1.7×10^{-2} cm^2/V, and S/μ are 168, 147 and 209 V/cm, respectively. This detector possesses one of the largest values of electron mobility-lifetime product among all values reported to date.

For surface A, the saturation photocurrents from different regions are almost identical, but $\mu\tau_b$ and S/μ values show more variability. Various regions of surface A were illuminated with 650-nm light. The best fits give $\mu\tau_b$ values of 1.1×10^{-2}, 2.1×10^{-2} and 2.8×10^{-2} cm^2/V, and S/μ are 96, 128 and 132 V/cm, respectively. Compared with surface B, surface A has smaller surface recombination velocities from the different regions. Thus, it is expected that the CZT detector with irradiation of surface A (as the cathode) will exhibit better detector performance than irradiation of surface B (as the cathode). Based on the alpha and gamma-ray responses, we

confirmed that surface A did indeed produce better detector performance. The surface recombination velocities extracted for surfaces A and B were based on the BM treatment. When the CZT detector is treated with 0.05-μm grit polishing without further BM chemical etching, the surface recombination velocity is two to three times higher than that treated with BM.

For the CZT detector illuminated with 800-nm light, it is anticipated that the surface recombination velocity is smaller than that with 650-nm light, since the penetration depth at 800 nm is larger than that at 650 nm. The $\mu\tau_b$ and S/μ values collected at different regions of surface A for 800-nm light illumination at a power of 70 nW. The two parameters are roughly independent of position, but slightly dependent on the incident light power. The surface recombination velocity tends to decrease with incremental illumination intensity for powers exceeding about 1.0 μW. For CZT irradiated with 900-nm light, the photon energy is insufficient to directly excite electron-hole pairs in the bulk. The process for generating free carriers is due to ionization of traps. [8] It is found that the experimental result can be well fit by the equation (solid line is the fit): [6]

$$I = 2I_0(\mu\tau_b V / L^2)\{1-(\mu\tau_b V / L^2)[(1-\exp(-L^2/(\mu\tau_b V))]\} \quad . \qquad (2)$$

The saturation current values (I_0) at different regions are quite different; however, the corresponding $\mu\tau_b$ values are roughly the same. At regions 3, 4 and 5, the values are 1.1×10^{-2}, 9.3×10^{-3} and 1.0×10^{-2} cm^2/V, respectively. It is worth noting that $\mu\tau_b$ values extracted from equation 2 are power dependent (i.e., the weaker the illumination, the higher the $\mu\tau_b$ value) [8]. The maximum $\mu\tau_b$ value corresponds to that obtained with 650 and 800 nm illumination.

In order to correlate the DC photoconductivity results with detector performance, the CZT detector was irradiated with an ^{241}Am gamma-ray point source. . Bromine-methanol-treated surfaces A and B were irradiated, and the charge collection efficiencies were measured as a function of the applied bias. The solid lines are theoretical fits with the Hecht equation for surfaces A and B. It is seen that with the BM treatment, the two charge collection curves are almost identical. The $\mu\tau$ values are 6.8×10^{-3} and 7.1×10^{-3} cm^2/V, respectively, for gamma-ray irradiation of surfaces B and A, respectively. The $\mu\tau$ value in the Hecht equation is an effective parameter to describe the charge collection. Here, $\mu\tau$ is a combination of a surface component and a bulk component, as described by the equation:[9]

$$\frac{1}{\mu\tau_{eff}} = \frac{1}{\mu\tau_b} + \frac{S}{\mu L}. \qquad (3)$$

Surface A has a slightly larger $\mu\tau$ value; therefore, it has a smaller surface recombination velocity.

The penetration depth of a 5.5-MeV alpha particle is much smaller compared to a 59.6-KeV gamma ray; thus, the alpha response of the detector reveals more information concerning the surface recombination velocity. Surface A was treated with BM, and for comparison charge collection efficiencies were measured for samples that were only mechanically polished. $\mu\tau$ values for the BM and polishing only treatments are 4.2×10^{-3} and 3.1×10^{-3} cm^2/V, respectively. It is clear that BM treatment corresponds to a smaller surface recombination velocity compared to no chemical etching. Using the $\mu\tau_b$ values taken from DC photoconductivity measurements (1.7×10^{-2} cm^2/V), the corresponding S/μ values extracted from equation 3 are 88 and 124 V/cm, respectively. These values are comparable to those obtained from the DC photoconductivity measurements.

The temperature dependence of $\mu\tau_b$ and S/μ has been measured on CZT detector 2, where the center of the detector was illuminated. Although the illumination intensity and wavelength were kept the same at different temperature, the photocurrents, which were relatively smaller than the leakage currents at room temperature, could be significantly larger than those at low temperature. It is seen that the leakage current of the sample decreases more than two orders of magnitude when temperature drops from 295 K to 250 K. Thus, it is anticipated that the electron lifetime and surface recombination velocity change accordingly. It is seen that the peak around 800 nm which associates with band gap of CZT crystal at 295 K shift towards low wavelength at 250 K; the normalized photocurrents excited with above band gap light are much lower than those at room temperature. Therefore, it is reasonable to believe that the surface recombination velocity at 250 K is larger than that at room temperature if a uniform electric field distribution approximation is still satisfied at this temperature. A relatively small photocurrent excited by below band gap light can be well distinguished from total current because the leakage current is smaller. Typical results of electron photocurrents illuminated with 900- nm light at a power of 5.8 nW and 940-nm at 81.0 nW . The corresponding $\mu\tau_b$ values are 3.5×10^{-3} and 2.9×10^{-3} cm^2/V, respectively. It is found that the $\mu\tau_b$ value has a tendency of decreasing with decrement of temperature.

c) Infrared imaging and Pockels effect in metal/CdZnTe/metal detectors

The infrared system has been developed and it is equipped with two cameras allowing several imaging modalities: (i) high spatial resolution CCD camera for imaging microscopic inhomogeneities such as tellurium rich second phase; (ii) a high sensitivity and dynamic range InGaAs CCD camera that allows us to perform Pockels measurements under flood illumination and further in the infrared than previously reported [10,11] and, (iii) infrared birefringence imaging. The latter has never been used for large size crystals as the ones studied here and for the first time allows us to identify the presence of "striae" on the size scale of approximately 1 mm and larger in crystal from most CZT manufacturer (Yinnel, Redlen, Orbotech) . Using reflection microscopy of rough polished surfaces we have ruled out that these features might be caused by the presence of twin grains. Possible causes leading to the formation of these striae are stress induced birefringence caused either by thermal stresses or dopant/defects ingomogeneities.

To further evaluate the quality of the crystals, measurements of alpha scanning and Pockels measurement have been performed. The setup is shown in Figure 5. With the present spatial resolution of these two measurements we have concluded that the effect of the striae is not apparent in the charge collection. These two measurement do show a drop in the internal electric field in the outer regions of the detector according to the equation [12]:

$$I(x,y) = I_0(x,y)\sin^2\left[\frac{\pi n_0^3 r_{41} L}{2\lambda} E(x,y)\right]$$

The above setup is being currently used in several CZT projects at Fisk including various national labs and industrial collaborators.

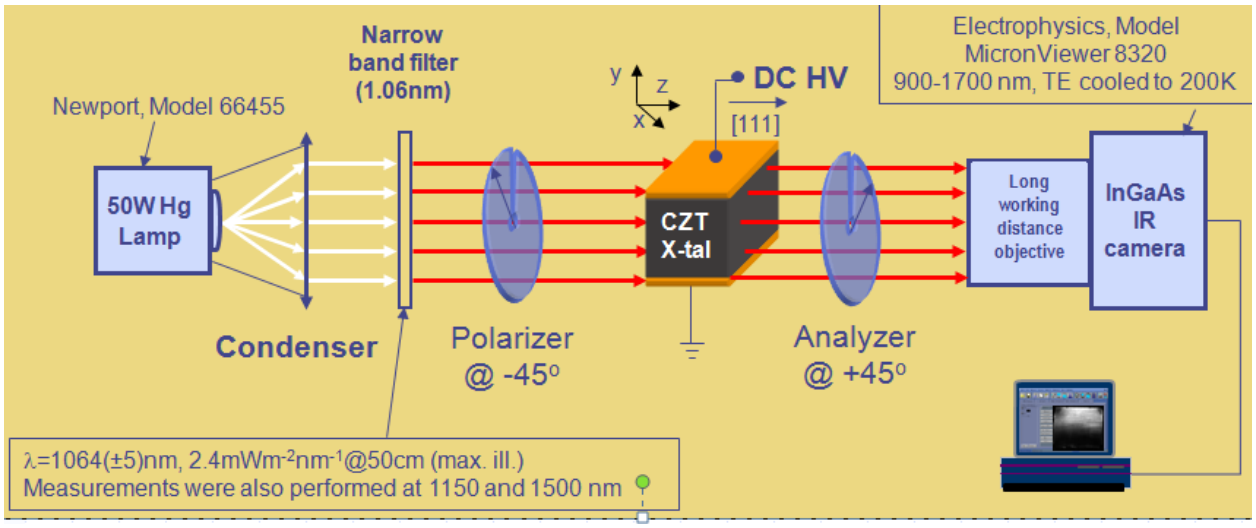

Figure 5. Experimental setup for Pockels and infrared birefringence imaging system

In conclusion, CZT detectors have a proven record for remote sensing applications, in particular for handheld devices that can be deployed for field applications. Although both the sensitivity and efficiency are still small and for wide-spread use price issues need to be resolved, CZT has important advantages over current scintillator technology, and no cooling is required compared with Ge detectors. We have studied the variation of electron mobility-lifetime product and surface recombination velocity on surface processing for $Cd_{1-x}Zn_xTe$ (CZT) radiation detectors. We found that the values for the electron mobility-lifetime product and surface recombination velocity depend on the polishing and chemical etching processes, and they are consistent for data taken using the DC photoconductivity and the detector response techniques.
Finally, we have been able to implement various surface and bulk characterization findings in implementing improved gamma ray spectrometers.

REFERENCES

1. J. E. Toney, B.A. Brunett, T.E. Schlesinger, R. B. James, and E. E. Eissler, IEEE Trans. Nucl. Sci. 44, 499(1997).
2. M. Amman, J. S. Lee, and P. N. Luke, J. Appl. Phys. 92, 3198 (2002).
3. B. W. Sturm, Z. He, T. H. Zurbuchen, and P. L. Koehn, IEEE Trans. Nucl. Sci, in press
4. A. Burger, H. Chen, K. Chattopadhyay, D. Shi, S. H. Morgan, W. E. Collins, and R. B. James, Nucl. Instr. and Meth. A428, 8(1999).
5. H. Chen, J. Tong, Z. Hu, D. T. Shi, G. H. Wu, K. -T. Chen, M. A. George, W. E. Collins, A. Burger, R. B. James, C. M. Stahle, and L. M. Bartlett, J. Appl. Phys. 80, 3509 (1996).
6. Y. Cui, M. Groza, D. Hillman, A. Burger, and R. B. James, J. Appl. Phys. 92, 2556 (2002).
7. A. Burger, H. Chen, J. Tong, D. Shi, M. A. George, K. -T. Chen, W. E. Collins, R. B. James, C. M. Stahle, and L. M. Bartlett, IEEE Trans. Nucl. Sci. 44, 934 (1997).
8. Y. Cui, M. Groza, A. Burger, and R. B. James, IEEE trans. Nucl. Sci. 51, 1172(2004).
9. Y. Cui, G. W. Wright, X. Ma, K. Chattopadhyay, R. B. James, and A. Burger, J. Electron. Mater. 30, 774 (2001).
10. De Antonis et al,IEEE Trans. Nucl. Sci. 43, (1996) 1487
11. Yao et al. Mat. Res. Soc. Symp. Proc. 449, 805-811 (1997)
12. R. Guenther, *Modern Optics*, (John Wiley & Sons, Inc. 1990), p. 569-590